

Quantum coherence and Kondo effect in multi quantum dot systems

Xi Dai

Department of Physics and Astronomy, Rutgers University, Piscataway, NJ 08854-8019

Tai-Kai Ng

Department of Physics, Hong Kong University of Science and Technology, Clear Water Bay, Kowloon, Hong Kong

(Dated: November 11, 2018)

The quantum interference effect among coupled identical quantum dots is studied in the present paper in the limit of strong intra-dot Coulomb interaction. When the average electron number in each dot is a fraction of an integer, quantum interference effect is greatly enhanced because of the sharing of extra electrons by multiple dots. We show that if the extra electron (hole) number is one, the low energy effective Hamiltonian can be map into the 2-channel $SU(M)$ Coqblin-Schrieffer model, where M is the total dot number. In particular, for two-dot system with odd number of total electrons, the model is equivalent to a two channel Kondo problem with anisotropic coupling between local spin and conduction bands. The more general situation with (arbitrary) fractional average electron number in each dot is also discussed. To study the Kondo effect, we apply the self consistent ladder approximation (SCLA) to study the electron spectral function for the two-dot system. Similar method is also used to study the triple-dot system where we show how quantum coherence manifest itself in the Aharonov-Bohm (AB) effect.

PACS numbers: PACS numbers: 74.25.Jb, 71.27.+a, 72.15.Qm, 73.63.Kv

Quantum interference effect among coupled quantum dots is becoming a very important problem because of its possible application in quantum computing[1] and has been studied widely both theoretically[4, 5, 6, 7] and experimentally[8, 9, 10]. Similar to single quantum dot, which are regarded as “artificial atoms”, the coupled quantum dots are viewed as “artificial molecules”[2]. The simplest way to model two coupled quantum dots is to treat the problem as a two-level system, where only one quantum level in each quantum dot is considered. When the quantum tunnelling term between the two dots is increased gradually, a transition from “ionic bonding” (where the electron is localized) to “covalent bonding” (where the electron is sheared by two dots) is expected[2]. In the latter case, the two energy levels will split to form bonding and anti-bonding states. This effect can be detected by photo emission measurement, where two delta peaks would appear right at the energies of the bonding and anti-bonding states. Unfortunately such a simple model is not applicable to real quantum dot systems, which contain many energy levels as well as strong coulomb interaction. In the present paper, we consider the opposite limit where the energy-level spacing within each dot is small and treat the energy levels in each dot in the continuum limit. This approximation is valid for temperature larger than the level spacing and is much closer to most real situations.

When M identical quantum dots are coupled by tunnelling processes, the total electron numbers in the system is a key factor determining the low energy physics of the system in the presence of strong coulomb interaction. If the total electron number equals $M \cdot N$, which is called the commensurate case, the configuration with the lowest charging energy is precisely N electrons per dot. Any tunnelling processes will cost two times of the charging energy and thus be suppressed in low temperature. Therefore the tunnelling term can be treated perturbatively and the coupling among quantum

dots can be viewed as “ionic bonding”. However the situation changes completely in the incommensurate case where the average electron number per dot is no longer an integer. In the present paper, we will focus on the simplest situation, where the total electron number equals $M \cdot N + 1$ (extra electron) or $M \cdot N - 1$ (extra hole). In this case we have M degenerate charging states with lowest energy. The i^{th} state ($i = 1, \dots, M$) has $N + 1$ ($N - 1$ for extra hole) electrons in the i^{th} dot and N electrons per dot in the rest of them. Turning on the quantum tunnelling terms will mix these M degenerate charging states non-perturbatively. The extra electron can be viewed as a “valence electron” of the system and a “covalent bond” is formed by equally sharing the “valence electron” by all the quantum dots in the ground state. This non-perturbative picture implies that perturbative treatment of the tunnelling term will break down in low temperature. We shall show that by projecting the Hamiltonian into the Hilbert space with the M lowest charging states, which is valid for $k_B T \ll$ the charging energy U , the M -dot problem can be mapped to a two-channel $SU(M)$ Coqblin-Schrieffer model where the physics of the system can be understood in analogy with Kondo physics. The Kondo temperature T_K is the energy scale below which quantum interference between quantum dots becomes important. At temperature well above T_K , quantum coherences between dots are lost and the charge dynamics between quantum dots are classic-resistor-like. At temperatures below T_K , the quantum interference effect builds up and a sharp coherence peak appears in the photo emission spectra, which is similar to the resonance peak in Kondo problem. By examining the Aharonov-Bohm (AB) effect in a three-dot system, we show that the coherent peak is associated with quantum coherent transport and can be interpret as a quasi-particle peak.

We start with the Hamiltonian for the M -dot system with

$M \cdot N + 1$ electrons,

$$H_{M-dot} = H_{cb} + H_0 + H_T \quad (1)$$

where

$$H_{cb} = U \sum_{\alpha=1}^M (\hat{n}_\alpha - n_0)^2 + V_{gate} \sum_{\alpha=1}^M \hat{n}_\alpha \quad (2)$$

is the coulomb blockade term with n_α being the particle number in the α^{th} dot, n_0 is the electron number of a neutral dot, and V_{gate} is the gate voltage applied to the multi-dot system to tune the chemical potential.

$$H_0 = \sum_{\alpha,k,\sigma} \epsilon_{\alpha k \sigma} C_{\alpha k \sigma}^+ C_{\alpha k \sigma} \quad (3)$$

and

$$H_T = \sum_{k,k',\sigma,\alpha,\beta} t_{k,k'} C_{\alpha k \sigma}^+ C_{\beta k' \sigma} + H.C. \quad (4)$$

are the kinetic energy of each quantum dot and tunnelling term between them, respectively. We note that similar Hamiltonian has been used to study the transport properties of coupled double-dot system by many authors[4, 6]. Here we include only the self-capacitance (Coulomb Blockade) term in our interaction term H_{cb} .

We shall map approximately our Hamiltonian to a quantum rotor Hamiltonian. The mapping is a generalization of the Matveev's mapping[11] of the single quantum dot Coulomb Blockade problem to the Kondo problem, and is valid when the total energy level number (N_{total}) and total number of electrons N satisfy $N_{total}, N \gg 1$. In the rotor notation, the Hamiltonian can be written as,

$$H_{Mdot} = U \sum_{\alpha=1}^M (\hat{L}_\alpha^z)^2 + V_{gate} \sum_{\alpha=1}^M \hat{L}_\alpha^z + \sum_{\alpha,k,\sigma} \epsilon_{\alpha k \sigma} f_{\alpha k \sigma}^+ f_{\alpha k \sigma} \\ + \sum_{k,k',\sigma,\alpha,\beta} t_{k,k'} f_{\alpha k \sigma}^+ f_{\beta k' \sigma} \hat{L}_\alpha^+ \hat{L}_\beta^- + H.C. \quad (5)$$

where \hat{L}_α^z is the angular momentum in z axis of a quantum rotor and represents physically the excess charge on dot α , $\hat{L}_\alpha^+, \hat{L}_\alpha^-$ are the raising and lowering operator of a quantum rotor. The physical electron operator at dot α is $C_{\alpha k \sigma}^+ = f_{\alpha k \sigma}^+ \hat{L}_\alpha^+$. The rotor representation is exact if M local constrains, $\sum_l f_{\alpha,l}^+ f_{\alpha,l} = n_0 + \hat{L}_\alpha^z$, for $i = 1, \dots, M$, are introduced to reproduce the correct Hilbert space. With $N_{total}, N \gg 1$, the above constrains can be treated in a large- N type expansion. In the large- N limit, the constraints are satisfied on average by properly choosing the chemical potential, the total fermion number on each dot has very small fluctuations.

If $V_{gate} = 0$, the ground state without tunnelling term is unique, corresponding to neutral dots with the fermion levels all filled up to the Fermi energy. In this case the quantum tunnelling term can be treated perturbatively because the

ground state is gaped. The quantum coherence between dots is very weak. By applying proper gate voltage we can shift the chemical potential such that states with total charge one are the lowest charging states. In this case we have M degenerate low energy states, corresponding to the excess electron located at M different dots. Since we are only interested in the low temperature region $k_B T \ll U$, we can safely neglect all the other charging states and project the above Hamiltonian to the subspace containing only the above M charging states. The projected Hamiltonian can be written as,

$$H_{eff} = \sum_{k,\alpha,\sigma} \epsilon_k f_{k\alpha\sigma}^+ f_{k\alpha\sigma} + t \sum_{kk',\alpha\beta,\sigma} f_{k\alpha\sigma}^+ f_{k'\beta\sigma} |\alpha\rangle \langle \beta| + H.C. \quad (6)$$

where $|\alpha\rangle$ represents a state with the extra electron on dot α . The above Hamiltonian can be viewed as a two channel $SU(M)$ Coqblin-Schiffer model. In double-dot case, it is also equivalent to two channel anisotropic Kondo mode[11, 12], where the two lowest energy charging states are equivalent to two pseudo spin states, up and down. Because of the presence of degenerate states, a perturbation series in $t_{k,k'}$ will diverge logarithmically at low temperature, reflecting the set up of quantum interference below the ‘‘Kondo Temperature’’ T_k , where the extra electron is allowed to hop around the quantum dots coherently forming a ‘‘covalent bond’’ solid including all M dots.

In the case with more than one extra electrons (holes), we obtain the following similar low energy effective model following the same procedure,

$$H_{eff} = \sum_{k,\alpha,\sigma} \epsilon_k f_{k\alpha\sigma}^+ f_{k\alpha\sigma} \\ + t \sum_{kk',\alpha\beta,\sigma} f_{k\alpha\sigma}^+ f_{k'\beta\sigma} D_{\alpha\beta}^{\gamma\delta} |\gamma\rangle \langle \delta| + H.C. \quad (7)$$

, where $D_{\alpha\beta}^{\gamma\delta} = \langle \gamma | \hat{L}_\alpha^+ \hat{L}_\beta^- | \delta \rangle$ and $\langle \gamma |, \langle \delta |$ denote all the degenerate charging states with the lowest energy. Notice that the number of degenerate states increases rapidly with more dots and extra electrons (holes). It is easy to see that Eq.7 reduces to Eq. 6 when the extra electron (hole) is limited to one. We will discuss the properties of this general model elsewhere.

In the following we shall apply the self consistent ladder approximation (SCLA) [12, 13, 14] to solve the above effective Hamiltonian for double- and triple- dots. The SCLA can be viewed as the generalization of the non-crossing approximation for the Kondo Hamiltonian and works very well in all temperature range in the two channel case. Recently the same method has been applied to the problem of charge fluctuation in a quantum box and the results are quite satisfactory compared with Bethe Ansatz.[12] Using the notation and diagrammatic rule in reference [14], the diagrams included by SCLA are shown in Fig.1, where the self energy of the charging state $|m\rangle$ is obtained from the irreducible T-matrix of

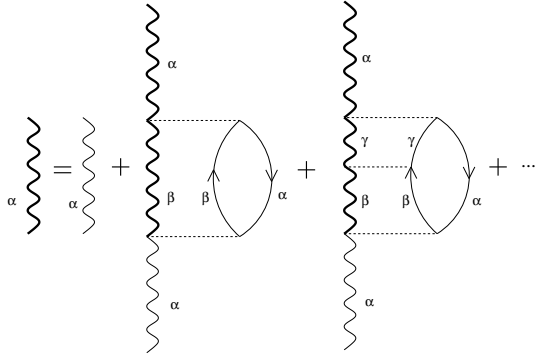


FIG. 1: (Color) The diagrams included in SCLA to calculate the renormalized Green's function of α th charging state. The thin and thick wave lines represent the bare and full Green's function of the α th charging state respectively. The solid lines represent the occupation number of fermions. And the dashed lines represent the interaction between fermions and local charging states.

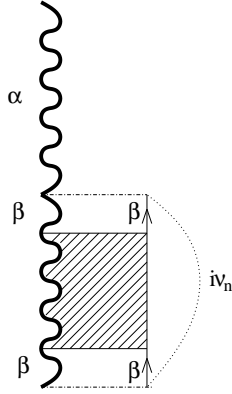


FIG. 2: The diagrams used to calculate physical electron Green's function. The dotted line represents the frequency carried by the green's function and the dot dashed lines represent the creation and annihilation of a physical electron. The shaded area represent all the ladder diagrams in Fig.1.

the charging states and fermions. The T-matrix is obtained by summing up all the ladder diagrams using the fully dressed Green's function of the charging states, which will close the self consistent integral equations. The SCLA integral equations were solved under different temperature iteratively and all the details can be found in reference[12, 13]. We shall first examine the electron spectral function in the two-dot system which can be seen directly in photo emission spectra.

$$G_{\sigma\alpha}(i\nu_n) = \sum_{l,l'} \int_0^\beta e^{i\nu_n\tau} \langle T L_\alpha^-(\tau) f_{l\sigma\alpha}(\tau) L_\alpha^+ f_{l'\sigma\alpha}^+ \rangle d\tau \quad (8)$$

To calculate the above Green's function, we have to include more charging states other than the ones with the lowest energy. Here we consider a double-dot system with $V_{gate} = 0.5$, $U = 1.0$, $N_l t = 4.0$, where N_l is the total number of levels in a single dot. A semi circle density of states with

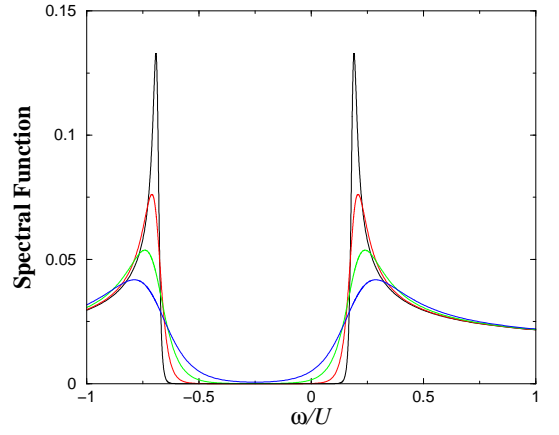


FIG. 3: The electronic spectral function for the double-dot system with temperature $T = 0.01, 0.05, 0.1, 0.2$, from the top to bottom.

half band width equals $D = 10.0$ is used as the density of states for a single dot. Following reference [12] we can estimate the Kondo temperature by $T_K = (2D\rho_0 t) \exp\left[-\frac{\pi}{4\rho_0 t}\right]$, which is 0.23 for the above parameters. Only the low energy charging states with total charge number equals $-1, 0, 1$ are considered to obtain the electron Green's function. The generalization of SCLA to include more charging states is quite straightforward. Since the total charge number is a good quantum number, we can simply apply the SCLA to the subspace with total charge number equals 1 and -1 , respectively by the above mapping and obtain the renormalized Green's function for each charging states. In the subspace with total charge zero, the charging state with the lowest energy is unique and the Green's function can be obtained by second order perturbation theory. Using the renormalized Green's function for the different charging states, the electron Green's function can be obtained following the diagrammatic rules in reference[14]. The diagram we used to calculate the electron Green's function is shown in Fig.2. The electron spectral function is shown in Fig.3. In high temperature, where the quantum interference effects are weak, a featureless spectra on top of the coulomb gap is found, which reflects the continuous energy levels inside each quantum dot. As temperature decreases, sharp resonance peaks which represent the "covalent bonding" states emerge gradually from the featureless continuum.

To study the quantum interference effect among the quantum dots more carefully, we examine the Aharonov-Bohm (AB) effect in the triple-dot system by connecting two leads to a three-dot system. In the weak lead-system coupling limit, we can treat the quantum tunnelling within the triple-dot system by SCLA and treat the lead-system tunnelling by first order perturbation. The Master's equation technique[15] is used to calculate the current flowing through the triple-dot system when a finite voltage is added between two leads. A magnetic flux enclosed by the dots can be included by introducing non trivial phase factors to the tunnelling terms between different quantum dots.

In Fig.4 we plot our results for the zero bias conductance as the function of gate voltage under different magnetic flux. The parameters we used here are $N_t t = 2.0, U = 1.0, D = 10.0$ and $T = 0.01$. We observe that the presence of the two resonance peaks in the electron spectral function, corresponding to transitions from charging state -1 to 0 and from 0 to 1 , is reflected in conductance measurement. The resonance peaks move to different gate voltages when magnetic flux changes, i.e. the quantum coherence manifest itself as a giant *magnetoresistance* effect at low temperature in the three-dot system which can be observed in transport measurements. We also plot the renormalized DC conductance as a function of magnetic flux in Fig.5 for gate voltage $V_g = 0.1$, $N_t t = 2.0, U = 1.0$ at different temperatures. At temperature $T = 0.01$ we can clearly see two resonance peaks corresponding to the resonance between charging states -1 to 0 and 0 to $+1$. The resonance feature disappears when the temperature is raised above the Kondo temperature T_K which is around 0.2 with our parameters. Notice that $g(\Phi)/g(0) \sim O(1)$ for temperature $\geq T_K$, consistent with the expectation that the system behaves like a classical resistor network at $T \geq T_K$.

We note that the quantum interference we studied in the present paper is a many-body effect which is established with the help of strong Coulomb interaction. The low temperature quantum coherent state is a covalent-bond solid state described by Kondo-type physics which is possible because of strong reduction in the number of low-energy charge excitations. This is contrary to the usual view where Coulomb interaction is considered as one of the origins of dephasing. It would be interesting to see how quantum coherence is modified at low temperature when Coulomb repulsion U decreases.

Summarizing, we show that quantum interference can be set up at low temperature between small particles where the Coulomb interaction is strong if the average electron numbers of the quantum dots are not an integer. The extra electrons behave like the valence electrons in molecular system to build the "covalent bonds" among quantum dots. For M coupled identical quantum dots with one extra charge, the low energy effective Hamiltonian is a two-channel $SU(M)$ Coqblin-Schrieffer model. In a two-dot system, the effective Hamiltonian is equivalent to a two channel Kondo model and quantum coherence will set up at temperatures lower than an effective "Kondo temperature". We compute the electronic spectral function using SCLA and sharp quasi particle peaks are found below the Kondo temperature. For triple-dot system the low energy effective Hamiltonian is 2-channel $SU(3)$ Coqblin-Schrieffer model and we can apply the same SCLA method to the problem. We study transports in the triple-dot system by the Master's equation technique. A strong AB effect is found below the "Kondo temperature" T_K indicating the presence of strong quantum coherence effect.

T.K. Ng thanks Hong Kong Research Grant Council for support through Grant no. HKUST6142/00P.

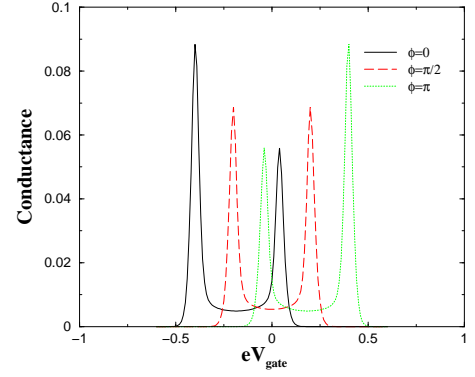


FIG. 4: (Color) The zero bias conductance as the function of gate voltage under different magnetic flux.

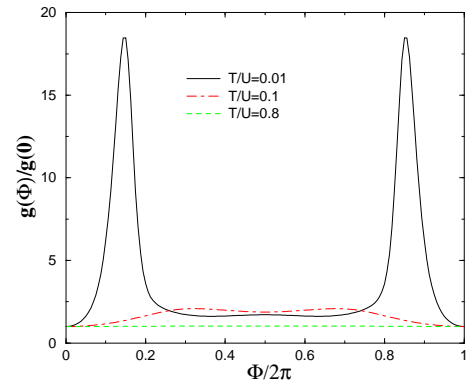


FIG. 5: (Color) The normalized DC conductance as the function of magnetic flux Φ .

-
- [1] D. Loss and D.P. DiVincenzo, Phys. Rev. A **57**, 120(1998).
 - [2] W.G. van der Wiel *et al.*, Rev. Mod. Phys. **75**, 1 (2003).
 - [3] X.X. Zhang *et al.*, Phys. Rev. Lett. **86**, 5562 (2001).
 - [4] J.M. Golden and B.I. Halperin, Phys. Rev. B **53**, 3893(1996).
 - [5] I.M. Ruzin *et al.*, Phys. Rev. B **45**, 13469 (1992).
 - [6] K.A. Matveev *et al.*, Phys. Rev. B **54**, 5637 (1996).
 - [7] W. Izumida and O. Sakai, Phys. Rev. B **62**, 10260 (2000).
 - [8] F.R. Waugh *et al.*, Phys. Rev. B **53**, 1413 (1996); F.R. Waugh *et al.*, Phys. Rev. Lett. **75**, 705 (1995).
 - [9] T. Fujisawa *et al.*, Science **282**, 932 (1998).
 - [10] T.H. Oosterkamp *et al.*, Nature **395**, 873 (1998).
 - [11] K. A. Matveev, Zh.Eksp. Teor. Fiz. **99**, 1598 (1991) [Sov. Phys. JETP **72**, 892 (1991)].
 - [12] E. Lebanon *et al.*, Phys. Rev. B **64**, 245338 (2001).
 - [13] S. Maekawa *et al.*, J. Phys. Soc. Jap. **54**, 1955 (1985).
 - [14] N.E. Bickers, Rev. Mod. Phys. **59**, 845 (1987).
 - [15] L.I. Glazman *et al.*, J. Phys.: Condens. Matter **1**, 5811 (1989); I.O. Kulik *et al.*, Sov. Phys.-JETP **41**, 308 (1975).